Ocean Engineering
September 2022, Volume 259 Pages 111800 (10p.)
https://doi.org/10.1016/j.oceaneng.2022.111800
https://archimer.ifremer.fr/doc/00786/89841/

Short and long term creep behaviour of polyamide ropes for mooring applications

Civier Laure [1, 2, 3, *], Chevillotte Yoan [1], Bles Guilhem [1], Montel Frédéric [1], Davies Peter [2, 3], Marco Yann [1]

[1] IRDL-UMR CNRS 6027, ENSTA Bretagne, 2 Rue François Verny, Brest, 29200, Bretagne, France
[2] IFREMER Centre Bretagne, Marine Structures Laboratory, 29280, Plouzané, France
[3] France Energies Marines, 525 Av. Alexis de Rochon, Plouzané, 29280, Bretagne, France

* Corresponding author : Laure Civier, email address : laure.civier@ensta-bretagne.org

Abstract :

Polyamide 6 fibres are of interest for mooring lines of floating wind turbines and these are continuously loaded throughout their service life. Such applications require the long term response of polyamide 6 ropes in water to be characterized. This paper presents results describing the long term creep behaviour of polyamide 6 sub-ropes with tests that lasted 2 years. A specially designed experimental set-up for long term creep test in water is presented first. Then, a kinetic study comparing creep and recovery is performed using a logarithmic identification of the strain rate. The need for performing long term creep tests is evaluated by comparing the long term creep results to those from short term creep tests lasting 3 h. The results show that a 3 h long creep test provides a reasonable prediction of long term creep strain using a single logarithmic linear law. Finally, a latch-based Weibull model is compared to a single linear logarithmic law to describe and predict creep and recovery response. It is shown that the Weibull model allows a better description of the recovery behaviour of polyamide 6 but is less well adapted for the description of creep.

Highlights

► Long-term creep experimental results of one and two years in water. ► A simple logarithmic law can predict the creep strain. ► Short-term creep tests can provide a good prediction of the long-term creep behavior.

Keywords : Polyamide 6, Creep, Water, Laid strand, Synthetic rope

.

1. Introduction

Floating wind platforms developed for marine renewable energies in shallow waters (between 50m and 100m) will be located in exposed areas where waves and wind are significant. The challenge for the sub-sea installations is to find a robust and suitable solution approved by the community that damps the dynamic loading for long-term applications. One proposed solution is a semi-taut mooring system with synthetic rope materials. The high compliance of synthetic ropes will lower the line tension and provide damping. This will lower the floater structural loads an—d bring more stability. The offshore industry already often prefers synthetic fibres ropes such as polyester compared to their metallic alternatives for deep offshore applications [7, 11, 26, 17]. Their high specific strength added to their flexibility and ease of handling are some of their key features. Polyester ropes are already used for mooring line applications in the oil & gas sector. The integrity of the system for floating wind turbines will be maintained by damping the dynamic loadings. For this purpose, it is necessary to have a compliant mooring system and so, the use of more stretchable fibre ropes than polyester is required. Aramid and HMPE are too stiff, small offsets result in very high tensions. Polyamide 6 is therefore of high interest for semi - taut mooring systems as it has a high elongation to rupture (up to 20%) and a low stiffness. It is also already used in other marine applications such as single point moorings for tankers, and it has a competitive price. Nevertheless, these mooring lines must last 20 years and limit the need for maintenance and re-tension procedures. Hence, they should show durability in terms of aging, fatigue life and creep. To use synthetic fibres with confidence, it is essential to characterize the visco-elasto-plastic behaviour which could be revealed as an increasing elongation with time under load (creep) or lower tension (after relaxation). Creep effects could impose modifying fairlead chains in the line or periodic re-tensionning [8]. Also, at high loads, creep rupture can occur though this can be prevented with adequate safety factors. Lastly, at high loads, creep effects can dominate the cyclic fatigue behaviour [8, 22]. At lower loads, the sensitivity of polyamide fibres to abrasion is the main cause of failure. New coatings have been developed to reduce the degradation due to abrasion between fibres [4, 27].

The following bibliographic section will discuss the literature on creep and recovery of fibres and fibres assemblies as well as on the existing models used for these phenomena then it will describe the existing experimental set-ups to test polyamide sub-ropes in water in creep and recovery.

1.1. Creep of fibres, fibre assemblies and ropes

Creep is defined as the strain under a constant load [21] and creep failure is considered as a static mechanism where the rope breaks after a certain duration at a constant load [4]. Mooring lines are subjected to almost constant load for most of their service life. Hence, the investigation of the creep mechanisms of fibres ropes is and has been a priority [6]. A typical curve of creep response of polymers is shown fig 1. Three different regimes are visible; primary creep of fibres occurs at low stresses and is recoverable when load is removed. During primary creep, the creep rate is high and it decreases when approaching the secondary creep. Secondary creep at higher stresses or longer times is non recoverable and shows a lower creep rate. The tertiary creep regime is the ultimate one before failure and can be identified with an increasing creep rate [21].

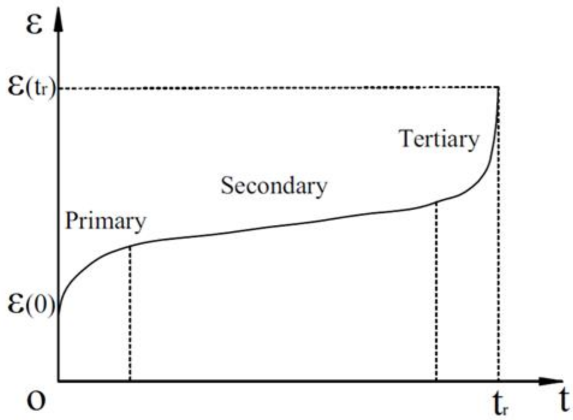

Figure 1: A typical strain–time curve in creep–rupture tests.

Studies of high tenacity and high modulus fibres for deep mooring lines are numerous, as the Oil and Gas sector has developed new solutions for their deepwater mooring lines [6]. Values for various fibres have been gathered in [21] and show that aramid fibres are the most resistant to creep followed by polyester fibres. Davies *et al* [8] presented a study of polyester creep behaviour. Creep tests were performed on fibres, yarns, sub-ropes and ropes. It was shown that polyester can be characterized by a linear evolution of the creep strain as a function of the logarithm of time. The creep rate of the sub-rope in water was evaluated at 0.10 %/decade. The creep was slowing with time on a logarithmic scale. A study of aramid fibres by Burgoyne [12] highlights that creep and recovery for aramid fibres could also be adequately described by a logarithmic time law and that the creep rate was dependent on the stress. High modulus polyethylene (HMPE) fibres are more sensitive to creep and creep rupture and are an exception; most HMPE fibres show a linear creep strain-time response though a recent grade has significantly reduced creep sensitivity [21, 24, 28]. Creep rupture on these fibres can occurs after around one hundred days at only 30% of their minimal breaking load (30 %MBL) [6, 19]. Polyamide fibres are a more flexible type of fibres than HMPE and show a large amount of primary creep (recoverable with time). Polyamide fibre can fail in less than a day at 50 %MBL load level [21]. Pal *et al* [24] studied braided polyamide 6,6 and obtained a total strain of 13.3% after 17 days of continuous loading at 32 %MBL. Instantaneous elongations were around 80% of the total elongation. However, polyamide 6 fibres exhibit lower creep rates than polyamide 66 [21]. Humeau *et al* [14] studied the influence of water on Polyamide 6 fibres and showed that they are very sensitive to water. Their behaviour is characterized by high water uptake and significant plasticity.

1.2. Creep models of different fibres

Many creep models have been proposed, using different types of approach. They are distinguished by the extent to which they take into account the fibre microstructure in their formulation [2].

A first category includes phenomenological models, which do not consider the molecular nature of individual fibres. The fibre is considered as an homogeneous (non) linear visco-elastic body [2]. Chailleux and Davies proposed a model with this approach using Shapery's generalized Boltzmann model integral combined with Perzyna's viscoplastic models to predict creep-recovery and long term creep behaviour of polyester mooring lines [3, 7]. Humeau *et al* [14] used the same approach to study creep at high loads on polyamide 6 yarns for both dry and immersed conditions. Schapery's model provided reasonable long-term predictions. Huang *et al* [13] employed Schapery's single integral model to describe the response of aramids and polyester fibres. Flory *et al* [10] also proposed a phenomenological model using a spring and dashpot. Chevillotte [4] adapted Flory's model to polyamide fibres using a multi-relaxation test to identify the parameters (figure 2). This model is phenomenological and describes short creep and recovery quite well.

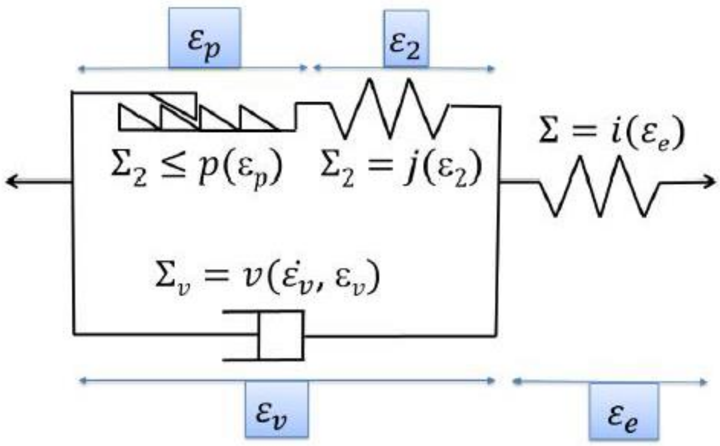

Figure 2: Behaviour law for polyamide 6 developed by Chevillotte and inspired by Flory's model using spring and dashpot [4]

Another approach by Fancey [9] suggested that the viscoelastic changes occur through incremental jumps, and this was used to describe primary and secondary creep regimes. The model is based on the Weibull distribution function. It was identified with a fit of experimental data on dry polyamide 6,6. The molecular mechanism envisaged was segments of molecules jumping between positions of relative stability. The expression for creep under applied load is:

$$\epsilon_c tot(t) = \epsilon_i + \epsilon_c \left[1 - \exp\left(-\left(\frac{t}{\eta_c}\right)^{\beta_c}\right)\right] \qquad (1)$$

Where ϵ_i is the initial instantaneous strain from application of the load and the ϵ_c function represents creep strain, which is determined by the characteristic life (η_c) and shape (β_c) as a function of the duration of loading, t [9]. The unloading phase is as well characterized by an elastic instantaneous strain recovery followed by time-dependent recovery:

$$\epsilon_r vis(t) = \epsilon_r \left[\exp\left(-\left(\frac{t}{\eta_r}\right)^{\beta_r}\right)\right] + \epsilon_f \qquad (2)$$

where the ϵ_r function, for viscoelastic strain recovery is determined by parameters similar to the creep function the ϵ_c and the ϵ_f the permanent strain from viscous flow.

1.3. Difficulties to study long term creep on polyamide 6 ropes

A complete study and understanding of cables is complicated by their multiscale nature. Each scale is contributing to creep differently and so, ideally, each scale should be characterized. Local scale tests allow us to identify the material (fibre) contribution, whereas macroscopic scale (sub-rope, rope) tests include the construction contributions to creep. Long term creep and creep rupture tests at higher scale than the filaments or yarns are not plentiful due to the technical challenges and cost. It requires a machine able to hold high loads for a long duration (months or years). To simulate the operational response of mooring lines, tests should be done in water. Water adds the constraint of keeping the water temperature quite constant for 2 years and measuring the local strain in water. Therefore, studies of creep in water are rare. One example is a study performed by Humeau on filaments, using dynamic mechanical analysis (DMA) equipment which controls the relative humidity [14]. Another difficulty is the attachments. The recommended terminations for ropes are splices. This imposes a long sample as splices have to be long enough to distribute the load uniformly inside the rope, without slipping. Due to high polyamide flexibility, the test machine must have a long stroke. A study on ropes described in [24] used a set-up consisting of hanging the rope with one end knotted on the iron bar of a 20 m high frame and the other end near the ground was knotted to the desired weight assembly.

To avoid the difficulties associated with long testing times, some research has focused on ageing the material with temperature using time-temperature equivalence [18, 19, 25] or higher loads by time-stress superposition [9].

The present paper describes a study of the long term creep behaviour of polyamide 6 sub-rope in water and examines the use of a simple model to fit the data. A comparison between creep and recovery kinetics is discussed. Short term creep tests were also performed, in order to conclude on the need to perform long term creep tests.

2. Materials and Methods

The synthetic fibre sub-ropes tested in the present study were made of polyamide-6 fibres and supplied by BEXCO, Hamme Belgium. The yarns used are supplied by *Nexis fibers* with a linear weight of 188 tex (g/km). The nylon rope samples used were specially manufactured for the research project and their linear density is 90 000 tex (g/km). The rope is a 1.80-meter-long (pin-to-pin) three-stranded rope of outer diameter around 12 millimeters, with eye-splices at each end. Each strand is composed of the 188 tex yarns twisted together into rope-yarns, which are themselves twisted together to form strands. The strand lay-length imposes splices of around 500 mm leaving a 800 mm central section. Eye-splices tighten the structure and stabilize the tension in each strand. A proprietary coating was applied on rope-yarns.

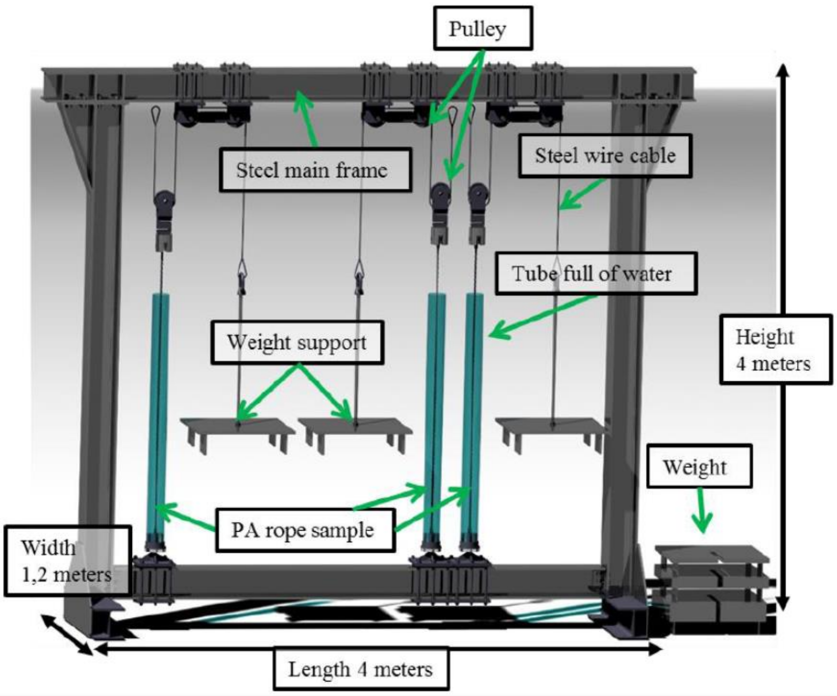

(a) Scheme of the long term Creep Test Frame

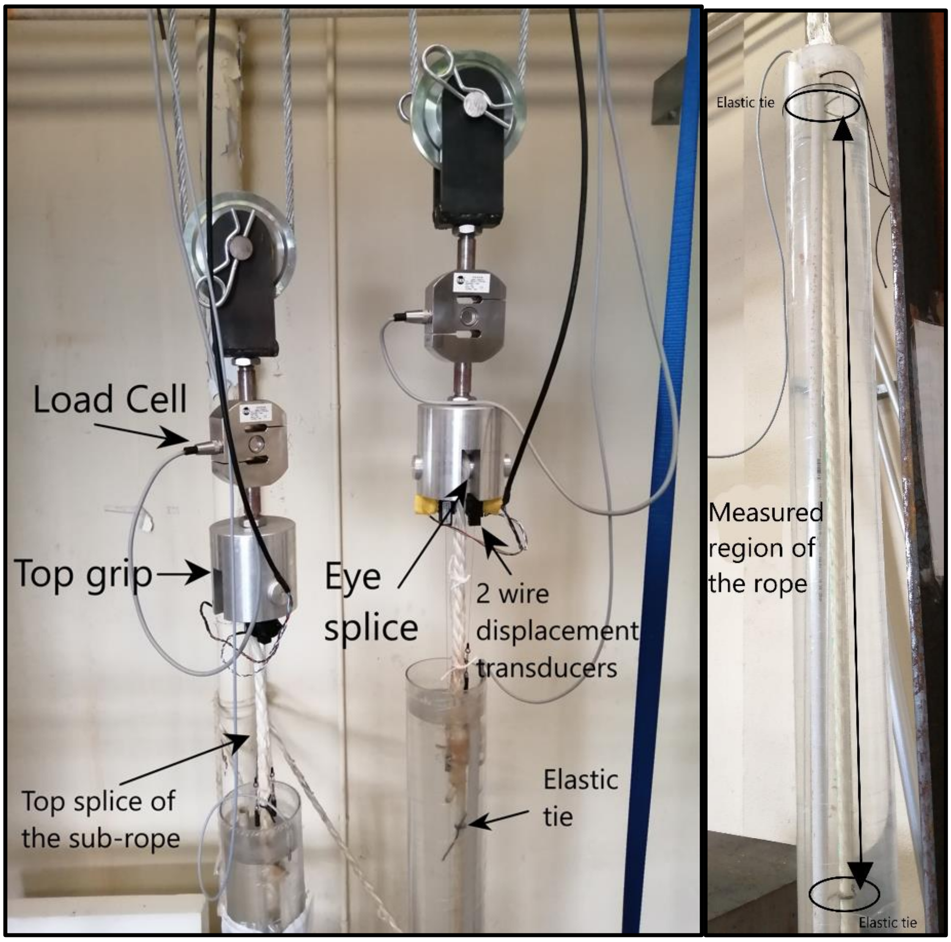

(b) Picture of the measurement system (c) Measured region of the rope

Figure 3: Long Creep Test Frame at ENSTA Bretagne [4]

This coating aims to reduce the abrasion inside the rope between rope-yarns improving the fatigue durability of polyamide sub-ropes. Tests have shown that it increases the lifetime of polyamide 6 rope significantly [5]. The supplier BEXCO indicated that the sub-rope minimum breaking tension load is 4T. Tension tests were performed on two samples to verify the supplier breaking value. The tension tests were performed at a mean speed of $3.05 \times 10^{-3}\ s^{-1}$ on a 20T Instron test machine. The breaking strength obtained was 42 kN for both samples, validating the supplier value. Hence, 40 kN will be used here as the minimum break load (MBL).

A specific test frame was designed and built for long term creep tests. It is a one piece steel module made of a linear vertical system with pulleys. The pulley system imposes a force on the sample, that is twice the steel weights (figure 3). To attach the splice termination to the machine, special grips with pins have been made. The pin diameter is 35 mm. Loads can be applied with modular steel blocks. These blocks slide on the support. The load is measured above each grip by a load sensor (FSB251 3000 DaN from Tei technologies). Samples are immersed for 10 hours before testing and then immersed in watertight tubes full of tap water. The water is directly pumped from a thermally controlled tank inside which the temperature is maintained around 20 ± 5 °C using three heaters (Eheim Jäger Thermocontrol™ 2048 100Watt). The water temperature of 20 ±5°C was set because it is an easy temperature to achieve throughout the year (different seasons) in Brest. It is also close to the mean ocean temperature (17.5°C). Higher temperatures could have been used to accelerate creep, but analysis of results would then require the multiplication of tests to determine acceleration factors, so for this series a representative temperature was preferred.

Table 1: Procedures for short and long term creep tests. (For the tests $LC45_B$, we performed a bedding-in (BI) sequence: 5.58 kN during 1h (0.042 days) followed by 1.8 kN during 1h)

	Creep phase				Recovery phase	
Test names	Load (kN)	Load (N/tex)	Load (%MBL)	Duration (days)	Unload (kN)	Duration (days)
$LC45_A$	18	0.20	45	0.16	/	/
$LC25$	9.9	0.11	25	424	1.08	414
$LC39$	15.750	0.175	39	838	/	/
$LC45_B$ *With BI*	5.58|1.08|18	0.062|0.012|0.20	14|2.7|45	0.042|0.042|405	1.08	433
$SC25$	9.9	0.11	25	0.125	1.08	0.125
$SC39$	15.750	0.175	39	0.125	1.08	0.125
$SC45$	18	0.20	45	0.125	1.08	0.125

The bottom grip enables the water flowing down the rope to be collected and returned to the tank. The temperature measured during the creep is presented in figure 4. Regulation was generally satisfactory during the two year test period except for two peaks; a cold one during 3 days in February 2021 and a hot one during four days in July. These temperatures variations did not have a visible effect on the creep curves. The elongation is measured using two wire displacement transducers attached to the top of the set-up (WPS-500-MK30-P10 and WPS-750-MK30-P10) fixed to the central part of the sub-rope at two points with 2mm diameter elastic ties. A minimal distance of at least 100 mm from the end of the splice was respected to fix the elastic ties so as not to be affected by the splices. The average length between the two measurement points was around 900 mm (figure 3.(c)). The elongation of the rope is defined as:

$$\Delta L = \frac{(C1 - C1_0) - (C2 - C2_0)}{L_0}$$

L_0 being the length between the two elastic ties taken after the 10 hours of immersion. $C1$ and $C2$ are the measures of the two wire displacement transducers. $C1_0$ and $C2_0$ are the values of the sensors when the length is L_0.
For the loading phase (beginning of the tests), the acquisition system was set with a high acquisition frequency (10 Hz) for one day. It was then changed to an acquisition rate better adapted to long term measurements: three acquisition periods per day of 10 minutes at 1 Hz. The acquisition system was shut down in between to be sure the sensor's conditioning would not be lost.

Short-term creep tests were performed at IFREMER on a servo-hydraulic machine with a load capacity of 300 ± 1 kN and a piston stroke of 3 meters. Samples were immersed for 5 hours before testing and sprayed with water during the tests. Samples were of exactly the same geometry as long term test samples. The strain in the section between splices was again determined using two wire displacement transducers (WS10-500-R1K-SB0-D8 and WS10-1000-R1K-SB0-D8) attached to points about 800 mm apart. The acquisition frequency was 2 Hz.

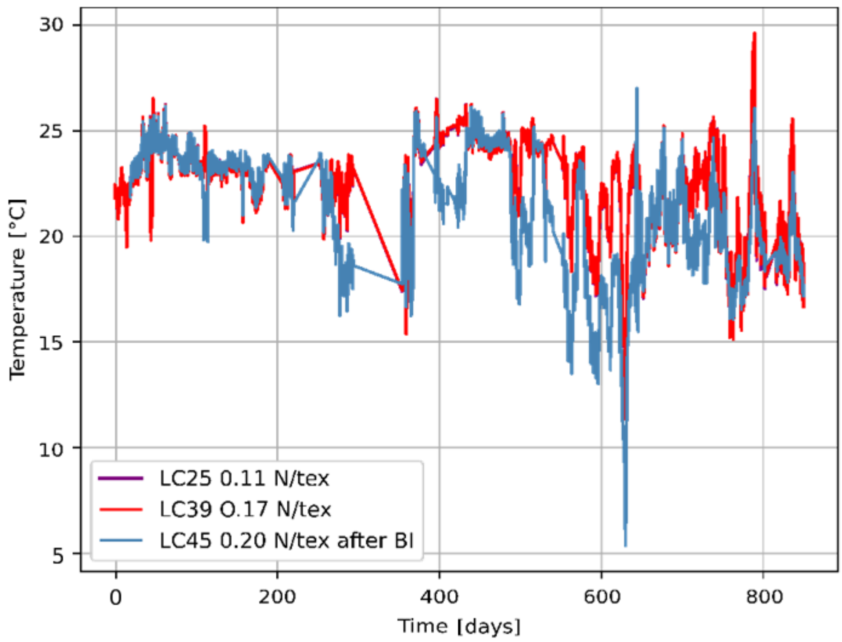

Figure 4: Measured Water Temperature inside the three tubes

The tests performed are presented in Table 1. The test $LC45_B$ was performed with a bedding-in procedure chosen following the recommendation of Bureau Veritas. The mean tension experienced by the floating wind turbine mooring lines is estimated at 15 %MBL. Hence, the bedding-in was chosen to be representative of these low loading conditions and does not follow the ISO recommendation [23]. The test $LC45_A$ is the same test but the sample did not undergo bedding-in. The comparison of these two tests allowed us to study the effect of the bedding-in (BI) procedure.

3. Stress and Strain definitions

The complex structure of synthetic fibre ropes complicates the use of the usual Cauchy stress based on the cross-section. A specific stress $\widetilde{\Sigma}$ based on the linear density of the rope is therefore used:

$$\widetilde{\Sigma} = \frac{\widetilde{T}}{\rho_t} \quad (3)$$

with ρ_t the density in kg/m³ and $\widetilde{\mathrm{T}}$ the Cauchy stress tensor in Pa.

In the 1D case (rope case), this specific stress leads to:

$$\Sigma = \frac{F}{\overline{\overline{\rho_t}}} \quad (4)$$

with $\overline{\overline{\rho_t}}$ the linear density in kg/m and F the tensile force in Newton.

The S.I. specific stress unit is N.m/kg (= J/kg). The textile sector uses rather a specific unit called N/tex with:

$$1\frac{N}{tex} = 10^6\,\frac{J}{kg} = 10^3\,\frac{Pa}{g/m^3} \quad (5)$$

where 1 tex = 1 g/km.

The logarithmic strain will be used for this study:

$$\epsilon_{log} = \log\left(\frac{l}{l_0}\right) \quad (6)$$

with L the current length, L_0 the reference length and $\log$ the natural logarithm.

4. Results and Discussion

4.1. Bedding-in first investigation

For many synthetic fibres ropes, a bedding-in protocol is applied in order to settle and stabilize the fibres and their geometry [1, 20, 29]. Such procedures can be difficult and expensive for large ropes but can ensure a better durability and control of the mooring lines. It is of importance to determine whether such a protocol will be needed for polyamide 6, and if so, which loading sequence would be suitable. Figure 5 presents the superposition of two creep tests at 45% MBL. One was performed with no bedding-in ($LC45_A$) and the other was preloaded and is referred to as $LC45_B$ in table 1.

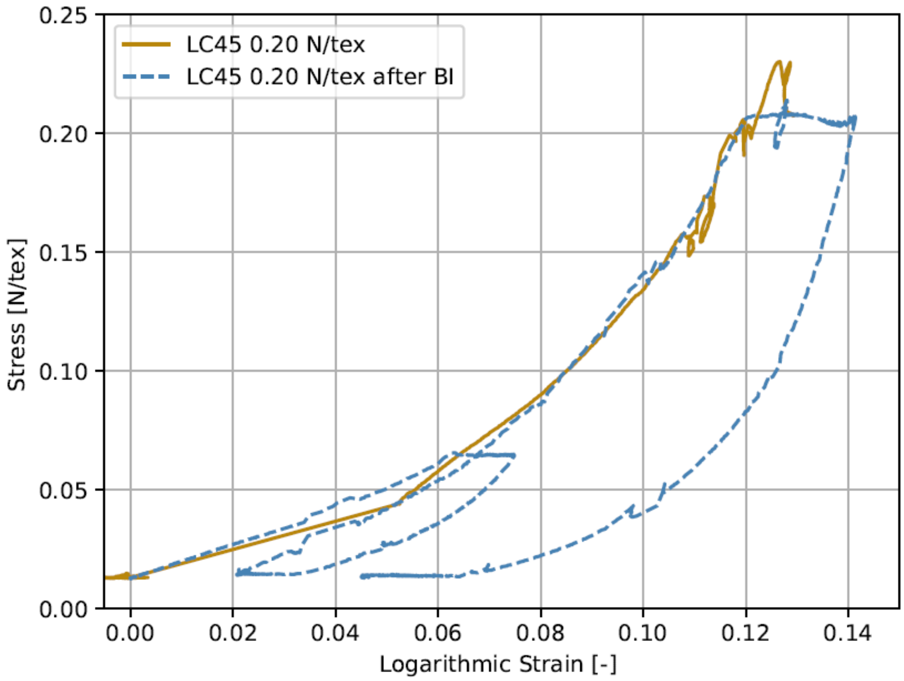

Figure 5: Stress in N/tex versus logarithmic strain of two tests at 45% MBL. The first one (continuous lines) being without a bedding-in procedure and the second one (dashed line) with a bedding-in procedure

The bedding-in procedure is detailed in table 1. The bedding-in procedure does not appear to have an impact during the subsequent loading phase of the sample. The plots are superposed even after the bedding-in. These results justify not applying a bedding-in procedure in the following comparison. However, other bedding-in protocols with higher loads might have an effect in the stabilization of the rope structure, and are being examined in current work.

4.2. Long term creep: Influence of the load

Long term creep tests in water were conducted on polyamide 6 sub-ropes for a two year period. The experimental data are presented in Figure 6 and 7.

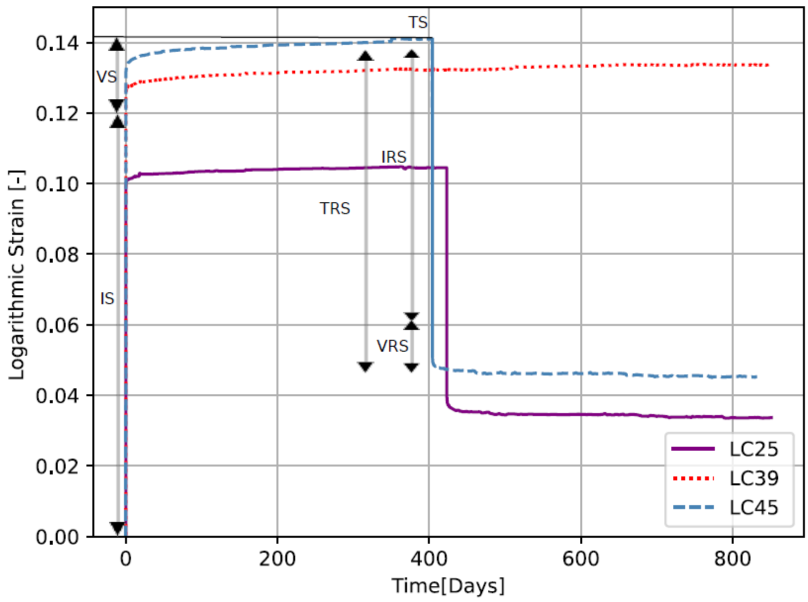

Figure 6: Long term creep and recovery results for three different loadings respectively 25%, 39% and 45% MBL

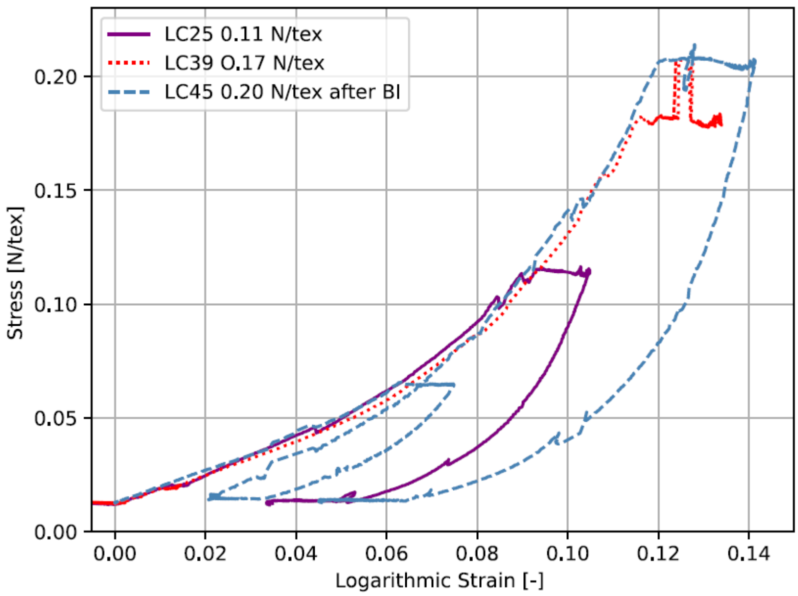

Figure 7: Stress [N/tex] versus logarithmic strain [/] of long term creep tests for three different loadings respectively 25%, 39% and 45% MBL

The peak we observe on the red dotted line curve LC39 on figure 7 was a local instability of the loading and did not impact the results (no corresponding peak on the strain results). Table 2 summarizes the measured instantaneous strain (IS), time-dependent (VS) strain and total strain (TS) during the loading (creep) and unloading (recovery) phases.

The load level has a clear effect. The creep and elastic strains increase with applied stress. The instantaneous strain values are around 85% to 90% of TS for all loads. The time-dependent values are around 10% to 15% of TS.

Table 2: Results of long and short Creep and Recovery Tests

Test	Loading phase				Recovery phase			
	Total duration (days)	TS (/)	IS (/)	VS (/)	Total duration (days)	TRS (/)	IRS (/)	VRS (/)
$LC25$	424	0.104	0.093	0.011	414	0.070	0.052	0.018
$LC39$	838	0.134	0.116	0.018	/	/	/	/
$LC45_B$	405	0.141	0.120	0.021	433	0.096	0.077	0.019
$SC25$	0.125	0.101	0.094	0.006	0.125	0.063	0.057	0.006
$SC39$	0.125	0.124	0.116	0.008	0.125	0.099	0.066	0.033
$SC45$	0.125	0.138	0.131	0.007	0.125	0.105	0.064	0.041

TS is the total strain; IS is the instantaneous strain, VS is the viscous strain

TRS, IRS and VRS are the same for recovery

On comparing the recovery between the samples at 25% and 45 %MBL, they recovered around 67% of TS and so, 33% of TS after creep has not been recovered. For LC25 and $LC45_B$, the instantaneous recovery is respectively 74% and 80% of the TRS and the time-dependent recovery is around respectively 26% and 20% of the TRS. The instantaneous strain is higher than the instantaneous recovery strain, meaning we may have modified the material during the loading phase leading to a permanent strain.

4.3. Kinetic study of creep and recovery

The curves in figure 8 confirm that polyamide 6 shows a logarithmic visco-elasto-plastic creep behaviour [15, 16]. The creep presents two phases. The primary phase goes from t_0 (beginning of the creep) to 10^{-2} days. From 10^{-2} days (around 15 minutes), we witness a stabilization of the creep rate. It becomes nearly linear as a function of the logarithm of time which could indicate the beginning of the secondary phase. The recovery presents three phases (figure 9): the first two phases are comparable to those of creep with a secondary phase following a linear evolution of the strain as a function of the logarithm of time. However, recovery rates seem to stabilize at the end of the test (fig 9).

We can fit the relationship between creep (and recovery) strain and time by the logarithmic law (for t > t_0):

$$\epsilon_c = A\, log_{10}\,(t - t_0) + \epsilon_0 \quad (7)$$

With A the logarithmic creep rate, t_0 the beginning of the creep (in days) taken when the load has reached a constant creep value and ϵ_0 the strain after one day of creep (at t_0 + 1day). This expression has the disadvantage of not being accurate for time close to t_0 but can be used for all other practical times. The logarithmic fits presented on figure 8 are determined using equation (7) identified on the data from 10^{-2} days up to the end of the experiment. The parameters t_0 and ϵ_0 are identified beforehand using the stress versus strain curve figure 7 to determine when the load became constant (beginning of creep). The parameter A is the slope of the logarithmic fit. Therefore, it is possible to model the creep using a single linear logarithmic law following equation (7) (fig 8).

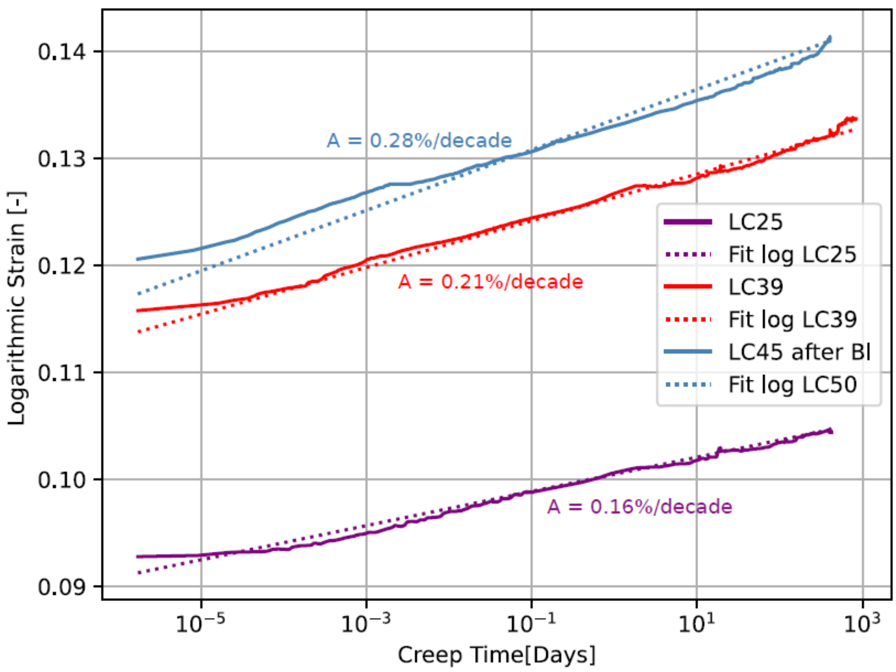

Figure 8: Long term creep strain versus logarithm of creep time for three different loadings respectively 25%, 39% and 45% MBL

Hence, we use a logarithmic identification for the creep rate:

$$A = \frac{\Delta \in}{\Delta log_{10}(t - t_0)} \quad (8)$$

To analyze the different phases in more detail, the creep rate was calculated for each decade of days and then smaller intervals were added for the last decade as it represents most of the creep duration. The measured creep and recovery rates are presented in Figures 10 and 11.

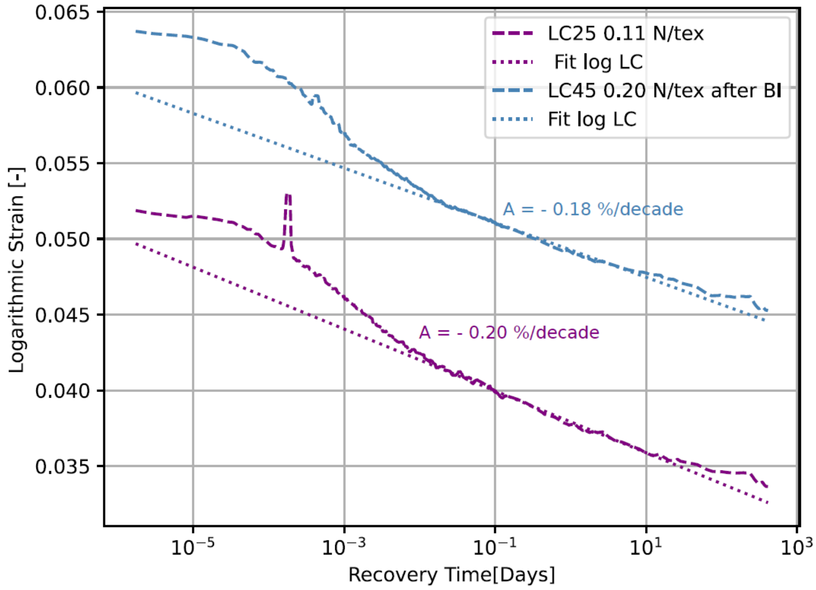

Figure 9: Recovery of the long term creep at 25% and 45% MBL

The creep and recovery rates are not smooth. This could be explained by the influence in the creep calculation of the instabilities of the measurements, which are especially likely to happen for long term experiments which are characterized by more perturbing events. Another explanation is that this may be due to damage inside the sub-rope or a sudden change in the construction of the rope. For example, increases in the creep rate values might be due to a "stick-slip" mechanism: the fibres go through creep slowly until they rearrange in a position that induces resistance (stick part). They then rearrange and produce a "slip" effect. The creep rate is sensitive to these types of variations because they can induce, locally, large increases in strain. The creep rate plot highlights the two phases mentioned above. There is a primary phase, between 0 and 10^{-2} days, where the creep rate is increasing. The second phase is located between 10^{-2} days and 100 days. This phase should present a stabilized logarithmic creep rate but is characterized by instabilities. If we note the creep scale, these variations remain small. Beyond 100 days of creep, the effect of the load is more visible with respectively for 25%, 39% and 45%, calculated rates of 0.2 %/decade, 0.3 %/decade and 0.35 %/decade. The creep rate values are almost proportional to the tension values.

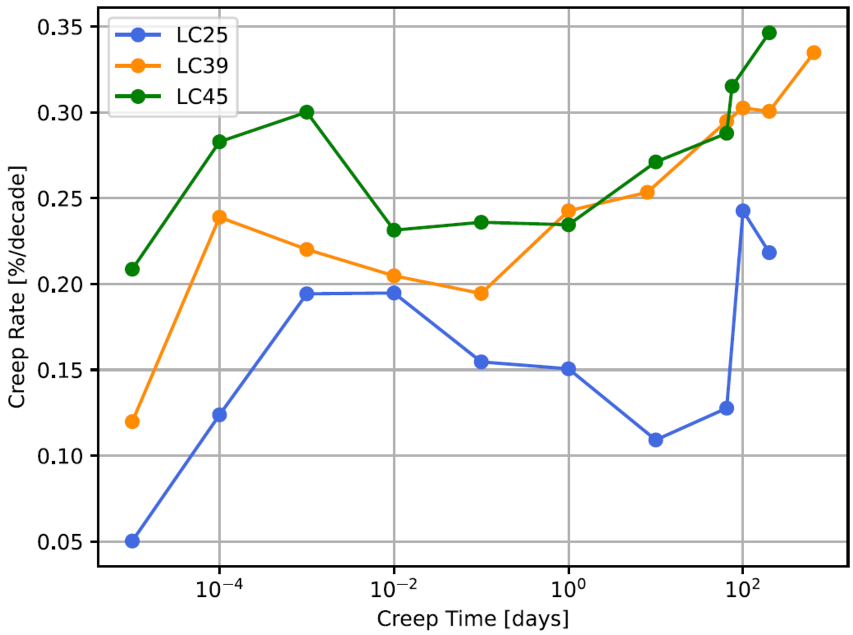

Figure 10: Creep rate in %/decade for the long term creep tests

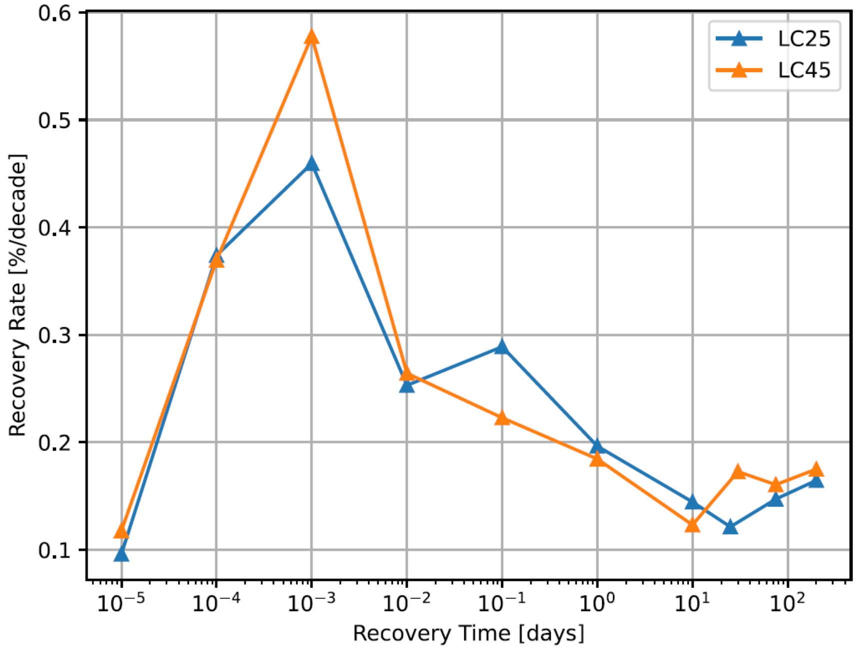

Figure 11: Absolute value of recovery rate in %/decade for the long term creep tests

The recovery rates also present three phases: the first one, between 0 and 10^{-2} days, is characterized by a fast recovery rate. It is followed by a decrease between 10^{-2} and 10^{1} days and maybe a stabilization from 10^{1} days to the end. Nonetheless, the recovery is still on-going and we did not reach a stable value of permanent strain. Comparing the initial values of creep and recovery rates (fig 10 and 11), the recovery is faster than the creep at the beginning.

4.4. Comparison of long and short term creep tests

Given the logarithmic evolution of the creep strain, it might be questioned whether long tests are necessary. The results obtained during an independent series of short term creep tests (3 hours) were therefore compared to those. The aim is to determine if we can predict long term creep strain with short term experiments. Figures 12 and 13 shows the results and figure 14 presents a superposition of the long and short term creep tests on a logarithmic time scale.

Table 3: Creep Rates from 10^{-2} days to the end of the creep test

	$LC25$	$LC39$	$LC45_B$	$SC25$	$SC39$	$SC45$
Rate %/decade	0.16	0.21	0.28	0.16	0.18	0.29

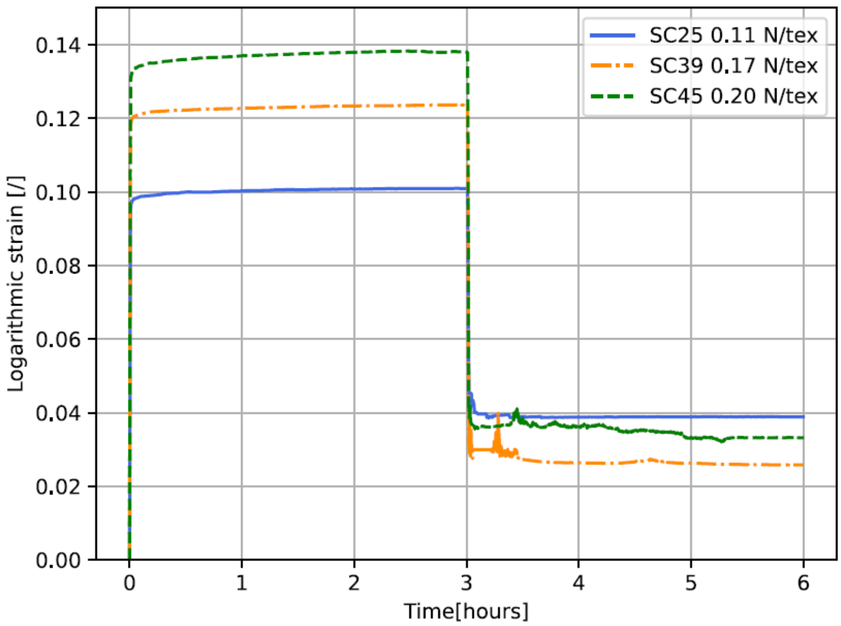

Figure 12: Short term creep and recovery results for three different loadings respectively 25%, 39% and 45% MBL

On figure 12, we can indeed observe many peaks. Unfortunately, these peaks appear to be caused by instabilities of the wire sensors when the sub-rope recovers. They may vibrate which gives a poor-quality signal. As the main aim of the study was to compare long and short-term creep, it was decided not to process this signal and to not use the first part of the short-term creep test recovery curve (SC25, SC39, SC45). Hence, the recovery analysis was only based on the final stabilized values obtained after 3 hours of recovery. These final values are not affected by the noise recorded between 3 and 4 hours. Efforts are being made to improve the measurement set up for future tests.

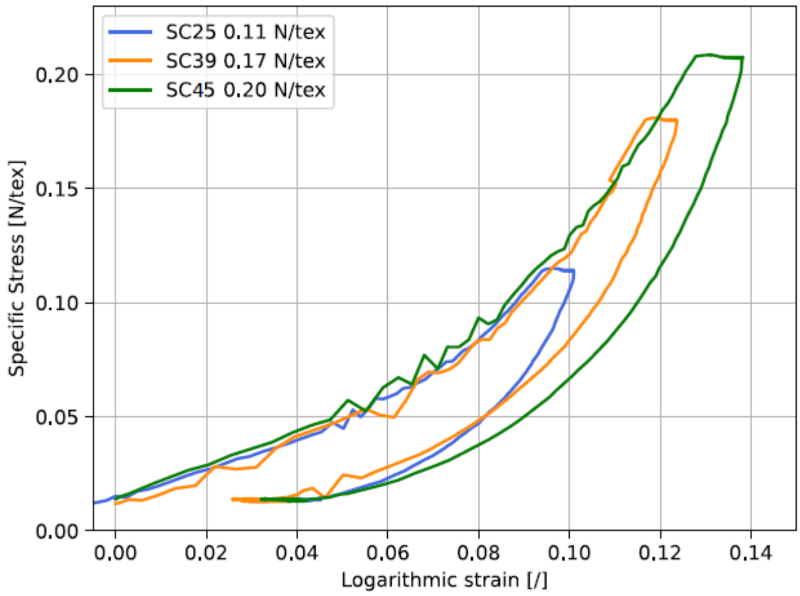

Figure 13: Stress [N/tex] versus logarithmic strain [/] of short term creep tests for three different loadings respectively 25%, 39% and 45% MBL

The total creep strains for short and long term creep are very similar. The small gap between the two seems to be due to the instantaneous response. These gaps could be explained by the variability between the samples (e.g. small differences in the splicing, which is a manual operation). It is observed from Table 2, that the instantaneous strain values (IS) are around ∼ 93% of TS and the viscous strain (VS) are ∼ 7% of TS for short term creep tests. As expected, the long term creep tests are characterized by a more important creep strain (around 10% to 15%). The instantaneous strain (IS) is not completely recovered by the instantaneous recovery strain (IRS).

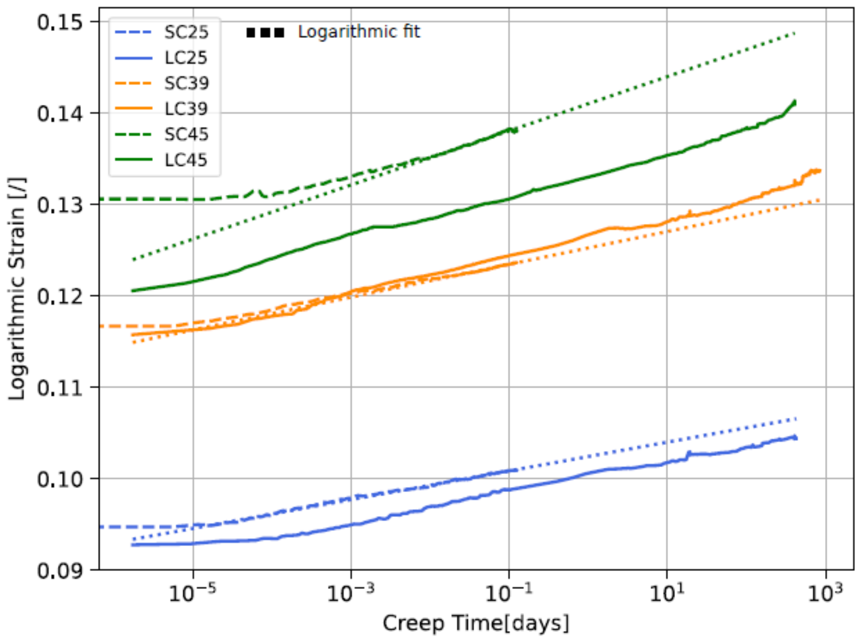

Figure 14: Superposition of long and short term creep strain in function of the logarithm of time with extrapolated short term creep logarithmic fit

The creep secondary phase reached at 10^{-2} days is visible on the short term creep tests (figure 14). Table 3 compares the values of creep rate A for a single logarithmic law fitted from 10^{-2} days to the end of the creep test. Extrapolation of the law identified on short term creep test indicates that a short term creep test of 3 hours could provide a good prediction of the creep happening in two years using a logarithmic linear law. For longer times, the creep rate may increase as a function of the load.

4.5. Model predictions

Fitting equations (1) and (2) to the data gives the results presented in table 4 and results are displayed, for creep, for the sample at 39 % MBL on figure 15 and, for recovery, for the sample at 25% MBL on figure 16.

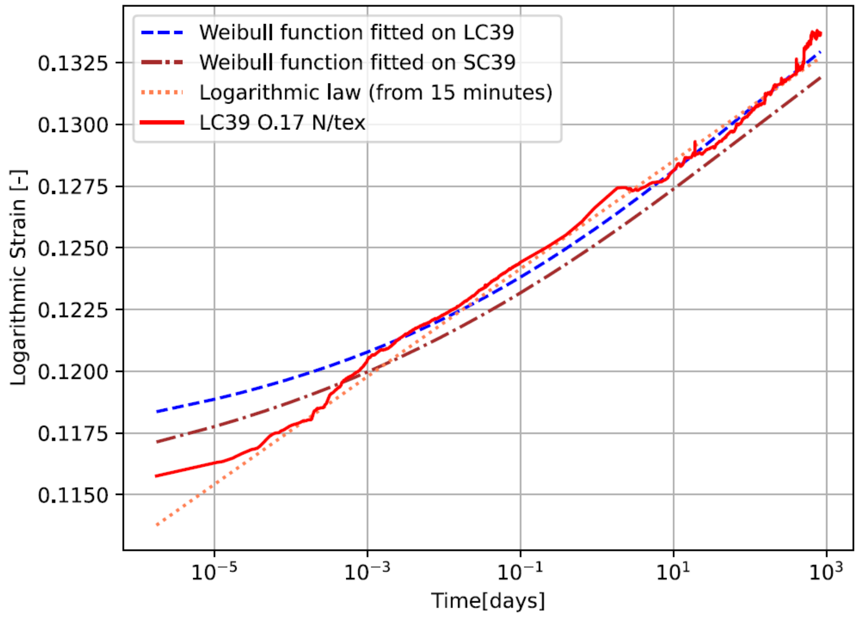

Figure 15: Weibull model fitted to the long term creep data LC39 at 39% MBL and to the short term creep SC39 at 39% MBL and comparison to a logarithmic law

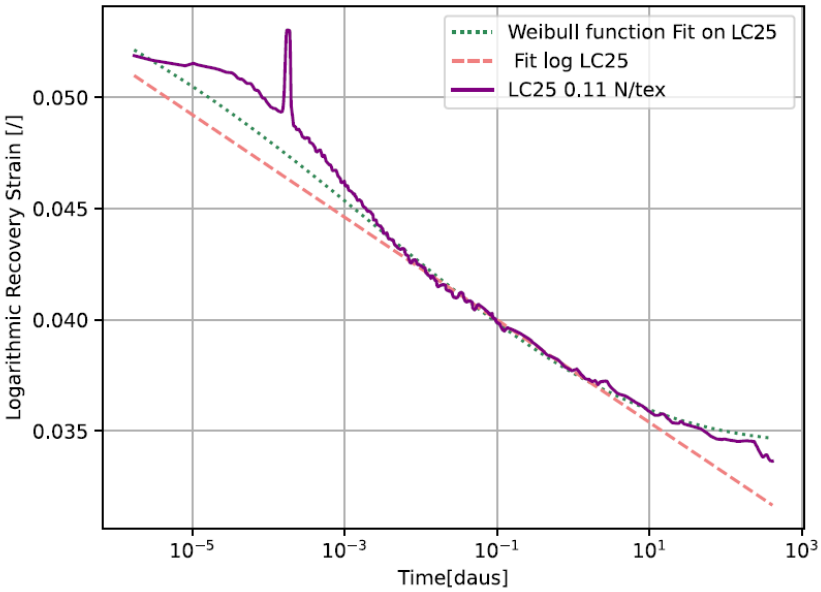

Figure 16: Weibull model fitted to the long term recovery data at 25% MBL and comparison to a logarithmic law

We observe that the Weibull function is not accurate to represent the beginning of creep. It may underestimate the importance of the reorganization of the structure in the primary phase. The result given by the Weibull model is close to the result obtained using a single logarithmic law identified from data between 10^{-2} days up to the creep end. Looking at the values of ϵ_c, both predict the creep contribution to be around 2% to 3%.

The creep strain increases with applied stress. In terms of a mechanical latch based spring and dashpot this may result from more time-dependent latch elements being activated under higher creep stresses [9]. The short term creep tests were fitted using the Weibull function to conclude on its ability to predict long term creep strain using short term creep tests. The obtained total strain after extrapolation is close to the long term creep value but does not take into account the strong increase at the end of the creep test. It was shown that a logarithmic linear law can accurately predict long term creep strain using short term creep tests (fig 15). The use of the Weibull function does not show any advantage for creep.

Table 4: Parameters obtained for Weibull model (equations (1) and (2))

Test name	$LC25$	$LC39$	$LC45_B$	$SC25$	$SC39$	$SC45$
Creep						
$\in_i$ $[-]$	0.089	0.16	0.117	0.091	0.114	0.127
$\in_c$ $[-]$	0.023	0.023	0.0346	0.024	0.025	0.037
η_c $[hours]$	2000	3000	2303	2169	2588	3120
β_c $[-]$	0.097	0.130	0.102	0.097	0.112	0.144
r $[-]$	0.992	0.998	0.999	0.989	0.993	0.986
Recovery						
$\in_r$ $[-]$	0.026	-	0.034	-	-	-
η_r $[hours]$	0.066	-	0.004	-	-	-
β_c $[-]$	0.13	-	0.11	-	-	-
$\in_f$ $[-]$	0.035	-	0.046	-	-	-
r $[-]$	0.981	-	0.978	-	-	-

However, the Weibull function fitted on the recovery data provides a better fit than the logarithmic law (figure 16) as it takes into account the decrease in the recovery rate with a shape parameter below unity. The viscous flow ϵ_f is predicted to be around 3% to 4% which would indicate we reached the permanent strain value expected by the model. However, the measured experimental recovery rate is not zero (fig 16) and so the permanent strain seems to not have been reached in the experimental data.

In service, the load is not always constant and the moorings may be subjected to cyclic amplitude variations due to waves or storms. Therefore, the identification of a model that takes into account the elasto-visco-plastic behaviour of the polyamide is needed.
Chevillotte [4] developed a 1D phenomenological model previously (figure 2). We also compared prediction from this model to the experimental data. The predicted creep strain stabilized at a constant value after 30 minutes of simulation. It was concluded that the model lacks relaxation times, so an integral model is now being investigated.

5. Conclusion

This paper presents experimental results to evaluate the long term creep properties of polyamide 6 mooring lines and to examine the necessity of running long term creep experiments. The main findings are:

1. The load level affects the creep behaviour. Higher loads will increase almost proportionally the creep strain values and the creep rate.
2. Both creep and recovery kinetics show three phases. The third phase of creep is characterized by an increase of the rate whereas for recovery, it is a stabilization of the rate. The recovery in the primary phase is faster than the creep.
3. Short term creep tests of up to 3 hours can provide a good prediction of long term creep behaviour using a logarithmic linear law up to 2 years.
4. A simple creep law can be used to describe the creep behaviour of polyamide 6 sub-ropes. A single logarithmic law identified using the data from the beginning of the secondary phases is accurate for creep but less for recovery. An approach using the Weibull function is more accurate for recovery and acceptable for creep though the beginning of the creep is not well described.

Further work will examine bedding-in procedures applying different loading sequences before creep. The influence of rope construction is also being evaluated, through tests on yarns, rope-yarns and strands.

5. Acknowledgements

This work was performed within the FEM/ANR POLYAMOOR and MONAMOOR projects of the research national french agency project (ANR-10-IEED-0006-16 and ANR-10-IEED-06-34, Investissements d'Avenir). This is led by France Energies Marines with partners Saipem, Bureau Veritas, BEXCO Ropes, ENSTA Bretagne, IFREMER, Naval Energies, Total Energies, University of Nantes, University Gustave Eiffel, NCD, IFSTTAR, GeM, CNRS, WEAMEC and RWE.

Thanks also to the engineering and technical staff team, without whom this study would not have been possible: Philippe Godec, Sébastien Bourc'his, Raphael Poncin, Didier Penchenat, Hervé Trebaol, Bruno Mecucci, Eric Saliou and Yannick Argouarc'h.

References

[1] Bain, C., Davies, P., Bles, G., Marco, Y., Barnet, J., 2020. Influence of bedding-in on the tensile performance of HMPE fiber ropes. Ocean Engineering 203, 107144. URL: https://linkinghub.elsevier.com/retrieve/pii/S0029801820302043, doi:10.1016/j.oceaneng.2020.107144.

[2] Bunsell, A., 2009. The chemistry, manufacture and tensile behaviour of polyester fibers., in: Handbook of tensile porperties of textile and technical fibres. woodhead publishing ed. Cambridge, England, pp. 223– 314.

[3] Chailleux, E., Davies, P., 2005. A Non-Linear Viscoelastic Viscoplastic Model for the Behaviour of Polyester Fibres. Mechanics of Time-Dependent Materials 9, 147–160. URL: http://link.springer.com/10.1007/s11043-005-1082-0, doi:10.1007/s11043-005-1082-0.

[4] Chevillotte, Y., 2020. Characterization of the long-term mechanical behavior and the durability of polyamide mooring ropes for floating wind turbines. Ph.D. thesis. ENSTA Bretagne. Brest.

[5] Chevillotte, Y., Marco, Y., Bles, G., Devos, K., Keryer, M., Arhant, M., Davies, P., 2020. Fatigue of improved polyamide mooring ropes for floating wind turbines. Ocean Engineering 199, 107011. URL:https://linkinghub.elsevier.com/retrieve/pii/S0029801820300883, doi:10.1016/j.oceaneng.2020.107011.

[6] Chimisso, F.E.G., 2009. Some experimental results regarding trial behavior on synthetic materials used to produce offshore morring ropes, in: Mechanics of Solids in Brazil 2009, Brazilian Society of Mechanical Sciences and Engineering. p. 12.

[7] Davies, P., Chailleux, E., Bunsell, A., Grosjean, F., Francois, M., 2003. Prediction of the long term behavior of synthetic mooring lines, OTC, Houston, Texas. pp. OTC–15379–MS. URL: https://onepetro.org/OTCONF/proceedings/03OTC/All-03OTC/Houston,%20Texas/34755, doi:10.4043/15379-MS.

[8] Davies, P., Huard, G., Grosjean, F., Francois, M., 2000. Creep and Relaxation of Polyester Mooring Lines, OTC, Houston, Texas. pp. OTC–12176–MS. URL:

https://onepetro.org/OTCONF/proceedings/00OTC/All-00OTC/Houston,%20Texas/40797, doi:10. 4043/12176-MS.

[9] Fancey, K.S., 2005. A mechanical model for creep, recovery and stress relaxation in polymeric materials. Journal of Materials Science 40, 4827–4831. URL: http://link.springer.com/10.1007/s10853-005-2020-x, doi:10.1007/s10853-005-2020-x.

[10] Flory, J., 2013. Cordage institute guidelines for marine grade nylon and polyester rope-making yarns. 2013 OCEANS - San Diego.

[11] Flory, J.F., Banfield, S.J., Berryman, C., 2007. Polyester Mooring Lines on Platforms and MODUs in Deep Water, OTC, Houston, Texas, U.S.A.. pp. OTC–18768–MS. URL: https://onepetro.org/OTCONF/proceedings/07OTC/All-07OTC/OTC-18768-MS/36927, doi:10.4043/ 18768-MS.

[12] Guimares, G.B., Burgoyne, C.J., 1992. Creep behaviour of a parallel-lay aramid rope. Journal of Materials Science 27, 2473–2489. URL: http://link.springer.com/10.1007/BF01105061, doi:10.1007/BF01105061.

[13] Huang, W., Liu, H., Lian, Y., Li, L., 2013.Modeling nonlinear creep and recovery behaviors of synthetic fiber ropes for deepwater moorings. Applied Ocean Research 39, 113– 120. URL: https://linkinghub.elsevier.com/retrieve/pii/S014111871200082X, doi:10.1016/j.apor.2012.10.004.

[14] Humeau, C., Davies, P., LeGac, P.Y., Jacquemin, F., 2018. Influence of water on the short and long term mechanical behaviour of polyamide 6 (nylon) fibres and yarns. Multiscale and Multidisciplinary Modeling, Experiments and Design 1, 317–327. URL: http://link.springer.com/10.1007/s41939-018-0036-6, doi:10.1007/s41939-018-0036-6.

[15] Hunt, D.G., Darlington, M.W., 1978. Accurate measurement of creep of nylon-6,6 at constant temperature and humidity. Polymer 19, 977–983. URL: https://linkinghub.elsevier.com/retrieve/pii/0032386178902094, doi:10.1016/0032-3861(78)90209-4.

[16] Hunt, D.G., Darlington, M.W., 1979. Prediction of creep of nylon-6,6 at constant stress, temperature and moisture content. Polymer 20, 241–246. URL:

https://linkinghub.elsevier.com/retrieve/pii/0032386179902283, doi:10.1016/0032-3861(79)90228-3.

[17] ISO 18692:2007(E), 2007. Fibre Ropes for offshore stationkeeping polyester. Standard. International Organization for Standardization. Geneva, CH.

[18] Lechat, C., 2011. Tensile and creep behaviour of polyethylene terephthalate and polyethylene naphthalate fibres. Journal of Materials Science 46,528–533. https://doi.org/10.1007/s10853-010-4999-x

[19] Lian, Y., Liu, H., Huang, W., Li, L., 2015. A creep–rupture model of synthetic fiber ropes for deepwater moorings based on thermodynamics. Applied Ocean Research 52, 234–244. URL: https://linkinghub.elsevier.com/retrieve/pii/S0141118715000838, doi:10.1016/j.apor.2015.06.009.

[20] Lian, Y., Liu, H., Li, L., Zhang, Y., 2018. An experimental investigation on the bedding-in behavior of synthetic fiber ropes. Ocean Engineering 160, 368–381. URL: https://linkinghub.elsevier.com/retrieve/pii/S0029801818305791, doi:10.1016/j.oceaneng.2018.04.071.

[21] MacKenna, H.A., Hearle, J.W.S., O'Hear, N., 2004. Handbook of fibre rope technology. Number 34 in Woodhead Publishing series in textiles, Woodhead, Cambridge.

[22] Mandell, J., 1987. Modeling of Marine Rope Fatigue Behavior. Textile Research Journal 57, 318–330. URL: http://journals.sagepub.com/doi/10.1177/004051758705700602, doi:10.1177/004051758705700602.

[23] NI 432 DT R02 E, 2018. Certification of fibre Ropes for Deepwater Offshore Services. Technical Report. Bureau Veritas.

[24] Pal, S.K., Thakare, V.B., Singh, G., 2007. Creep behaviour of braided cordages made of high performance fibres for aerospace applications. Indian J. Fibre Text. Res. , 8.

[25] Pang, J.W., Fancey, K.S., 2006. An investigation into the long-term viscoelastic recovery of Nylon 6,6 fibres through accelerated ageing. Materials Science and Engineering: A 431, 100– 105. URL: https://linkinghub.elsevier.com/retrieve/pii/S0921509306008495, doi:10.1016/j.msea.2006.05.052.

[26] Petruska, D., Geyer, J., Macon, R., Craig, M., Ran, A., Schulz, N., 2005. Polyester mooring for the Mad Dog spar—design issues and other considerations.Ocean Engineering 32, 767– 782. URL: https://linkinghub.elsevier.com/retrieve/pii/S0029801804002070, doi:10.1016/j.oceaneng.2004.10.002.

[27] Ridge, I.M.L., Banfield, S.J., Mackay, J., 2010. Nylon fibre rope moorings for wave energy converters, in: OCEANS 2010 MTS/IEEE SEATTLE, IEEE, Seattle, WA. pp. 1–10. URL: http://ieeexplore.ieee.org/document/5663836/, doi:10.1109/OCEANS.2010.5663836.

[28] Vlasblom, M., Boesten, J., Leite, S., Davies, P., 2012. Creep and stiffness of HMPE fiber for permanent deepwater offshore mooring. doi:10.1109/ OCEANS-Yeosu.2012.6263399. pages: 7.

[29] Weller, S., Davies, P., Vickers, A., Johanning, L., 2014. Synthetic rope responses in the context of load history: Operational performance. Ocean Engineering 83, 111–124. URL: https://linkinghub.elsevier.com/retrieve/pii/S0029801814000912, doi:10.1016/j.oceaneng.2014.03.010.